

Superconductivity from perturbative one-gluon exchange in high density quark matter

Thomas Schäfer* and Frank Wilczek†

School of Natural Sciences

Institute for Advanced Study

Princeton, NJ 08540

Abstract

We study color superconductivity in QCD at asymptotically large chemical potential. In this limit, pairing is dominated by perturbative one-gluon exchange. We derive the Eliashberg equation for the pairing gap and solve this equation numerically. Taking into account both magnetic and electric gluon exchanges, we find $\Delta \sim g^{-5} \exp(-c/g)$ with $c = 3\pi^2/\sqrt{2}$, verifying a recent result by Son. For chemical potentials that are of physical interest, $\mu < 1$ GeV, the calculation ceases to be reliable quantitatively, but our results suggest that the gap can be as large as 100 MeV.

*Research supported in part by NSF PHY-9513835. e-mail: schaefer@sns.ias.edu

†Research supported in part by DOE grant DE-FG02-90ER40542. e-mail: wilczek@sns.ias.edu

1. The behavior of matter at very high baryon density but small temperature is of interest in connection with the physics of neutron stars and heavy ion collisions in the baryon rich regime. Moreover, it has been realized that matter at very high density exhibits many non-perturbative phenomena, such as a mass gap and chiral symmetry breaking, in a regime where the coupling is weak and systematic calculations are possible.

At very high density the natural starting point is a Fermi sphere of quarks. The corresponding low energy excitations are quasiparticles and holes in the vicinity of the Fermi surface. Since the Fermi momentum is large, asymptotic freedom implies that the interaction between quasiparticles is weak. However, as we know from the theory of superconductivity, the Fermi surface is unstable in the presence of even an arbitrarily weak attractive interaction. In QCD, the attraction is provided by one-gluon exchange between quarks in a color anti-symmetric $\bar{3}$ state. QCD at high density is therefore expected to be a color superconductor [1,2].

A particularly interesting case is QCD with three flavors. In this case the most favorable type of pairing involves the coupling of color and flavor degrees of freedom, color-flavor-locking [3]. This implies, among other things, that all gluons acquire a mass and that chiral symmetry is broken. We have argued that in the color-flavor-locked phase not only universal features, in particular the symmetry breaking pattern, but also many non-universal properties, such as the spectrum of low-lying states, exactly match the expectations for hadronic matter at low baryon density [4]. This means that nuclear matter at low density might be continuously connected to quark matter at high density, without any phase transition.

It also means that at very high density many interesting properties of hadronic matter, such as the magnitude of the chiral condensate, can be calculated in weak coupling perturbation theory. The first step in such a program is the calculation of the superconducting gap. This calculation was first attempted by Bailin and Love [5]. They used a schematic IR cutoff in the gluon propagator. In their treatment, the gap is of the form $\Delta \sim \mu \exp(-c/g^2)$, where c depends logarithmically on the IR cutoff. Recently, the problem was revisited by Son [6], who argued that the gap is dominated by magnetic gluon exchanges, and that the infrared

behavior is regulated by dynamic screening. He obtained $\Delta \sim \mu g^{-5} \exp(-3\pi^2/(\sqrt{2}g))$.

Our purpose in the present work is to rederive and strengthen this result, and to determine the overall numerical coefficient.

2. In order to derive a gap equation, we follow the standard Nambu-Gorkov formalism and introduce a two component field $\Psi = (\psi, \bar{\psi}^T)$. The inverse quark propagator takes the form

$$S^{-1}(q) = \begin{pmatrix} \not{q} + \not{k} - m & \bar{\Delta} \\ \Delta & (\not{q} - \not{k} + m)^T \end{pmatrix}, \quad (1)$$

where $\bar{\Delta} = \gamma_0 \Delta^\dagger \gamma_0$. The gap is a matrix in color, isospin, and Dirac space. In the following we consider the case of two massless flavors. We will assume that the gap is anti-symmetric in both flavor and color, and has total angular momentum zero. In the case of short range interactions, this assumption can be justified from our study of the renormalization group equations for a general four-fermion interaction [7,8]. The one-gluon exchange interaction is long range, and other forms of pairing might take place. In particular, since the interaction is dominated by almost collinear scattering, one might expect higher partial waves to play a role [6]. In the following, we will concentrate on the total angular momentum zero gap.

We also assume that the gap has positive parity. One-gluon exchange does not distinguish between pairs of positive or negative parity [9]. This degeneracy is lifted by instantons, which favor the positive parity channel [10,11,7]. At large chemical potential instanton effects are exponentially suppressed. In the following, we will therefore assume that the only instanton effect is to determine the parity of the gap.

In addition to that, we neglect quark mass effects and chiral symmetry breaking LR condensates. As shown in [7] there is no BCS instability in the case of pairing between left and right handed quarks. The formation of LR condensates is therefore suppressed by m/μ . The form of the gap matrix is then [12]

$$\Delta_{ij}^{ab}(q) = (\lambda_2)^{ab} (\tau_2)_{ij} C \gamma_5 (\Delta_1(q_0)(1 + \vec{\alpha} \cdot \hat{q}) + \Delta_2(q_0)(1 - \vec{\alpha} \cdot \hat{q})). \quad (2)$$

In the weak coupling limit, we can replace $\vec{\alpha} \cdot \hat{q}$ by the unit matrix using the equations

of motion. In this limit, only Δ_1 survives. We will see this explicitly from the solution of the gap equation presented below. We have neglected the dependence of the gap on the magnitude of the momentum, but kept the dependence on frequency. The dependence on momentum can be dropped because, in the weak coupling limit, all momenta are close to the Fermi surface. For short range interactions, the dependence on frequency can also be neglected. This is not the case here. Because long range interactions are important, retardation effects cannot be neglected.

The self energy in the Nambu-Gorkov formalism obeys the Dyson-Schwinger equation [5]

$$\Sigma(k) = -g^2 \int \frac{d^4q}{(2\pi)^4} \Gamma_\mu^a S(q) \Gamma_\nu^b D_{\mu\nu}^{ab}(q-k). \quad (3)$$

Here, $\Sigma(k) = -(S^{-1}(k) - S_0^{-1}(k))$ is the proper self energy, Γ_μ^a is the quark-gluon vertex and $D_{\mu\nu}^{ab}(q-k)$ is the gluon propagator. To leading order in the perturbative expansion, we can use the free vertex

$$\Gamma_\mu^a = \begin{pmatrix} \gamma_\mu \lambda^a / 2 & 0 \\ 0 & (\gamma_\mu \lambda^a / 2)^T \end{pmatrix}. \quad (4)$$

We will study the importance of vertex corrections below. To leading order, we can also neglect the diagonal part of the proper self energy, that is the fermion wave function renormalization [6]. In this case, (3) reduces to an equation for the gap matrix,

$$\Delta(k) = -g^2 \int \frac{d^4q}{(2\pi)^4} \left(\gamma_\mu \frac{\lambda^a}{2} \right) S_{21}(q) \left(\gamma_\nu \frac{\lambda^a}{2} \right)^T D_{\mu\nu}(q-k). \quad (5)$$

Here, $S_{21}(q)$ is the 21-component of the fermion propagator in the Gorkov representation. $S_{12}(q)$ is determined from the inverse of (1). We have

$$S_{21}(q) = \frac{1}{(\not{q} - \not{\mu})^T} \Delta \frac{1}{(\not{q} + \not{\mu}) + \bar{\Delta} [(\not{q} - \not{\mu})^T]^{-1} \Delta}. \quad (6)$$

Inserting the ansatz (2) for the gap gives

$$S_{21}(q) = (\lambda_2 \tau_2 C \gamma_5) \left(\frac{\Delta_1 (1 - \vec{\alpha} \cdot \vec{q})}{q_0^2 - (|\vec{q}| - \mu)^2 - \Delta_1^2} + \frac{\Delta_2 (1 + \vec{\alpha} \cdot \vec{q})}{q_0^2 - (|\vec{q}| + \mu)^2 - \Delta_2^2} \right). \quad (7)$$

Both the RHS and the LHS of the gap equation are proportional to τ_2 , so the flavor structure simply drops out. The color coefficient is given by

$$c = \frac{1}{4}(\lambda^a)^T \lambda^2 \lambda^a = -\frac{N_c + 1}{2N_c} \lambda^2 = -\frac{2}{3} \lambda^2 \quad (N_c = 3), \quad (8)$$

where we have used the Fierz identity $(\lambda^a)_{ij}(\lambda^a)_{kl} = -2/N_c \delta_{ij} \delta_{kl} + 2\delta_{il} \delta_{jk}$ and the factor $1/4$ comes from the color generators $t^a = \lambda^a/2$. Projecting (5) on $\Delta_{1,2}$ gives two coupled gap equations

$$\Delta_{1,2}(k_0) = \frac{2g^2}{3} \int \frac{d^4q}{(2\pi)^4} \left\{ \text{tr} \left(\gamma_\mu (1 - \vec{\alpha} \cdot \hat{q}) \gamma_\nu (1 \pm \vec{\alpha} \cdot \hat{k}) \right) \frac{\Delta_1(q_0)}{q_0^2 - (|\vec{q}| - \mu)^2 - \Delta_1(q_0)^2} \right. \\ \left. + \text{tr} \left(\gamma_\mu (1 + \vec{\alpha} \cdot \hat{q}) \gamma_\nu (1 \pm \vec{\alpha} \cdot \hat{k}) \right) \frac{\Delta_2(q_0)}{q_0^2 - (|\vec{q}| + \mu)^2 - \Delta_2(q_0)^2} \right\} D_{\mu\nu}(k - q), \quad (9)$$

where the two signs of $\vec{\alpha} \cdot \hat{k}$ on the RHS correspond to Δ_1 and Δ_2 on the LHS.

We now must specify the gluon propagator. The gluon propagator in a general covariant gauge is given by

$$D_{\mu\nu}(q) = \frac{iP_{\mu\nu}^T}{q^2 - G} + \frac{iP_{\mu\nu}^L}{q^2 - F} + \xi \frac{iq_\mu q_\nu}{q^4} \quad (10)$$

where D and F are functions of q_0 and $|\vec{q}|$ and the projectors $P_{\mu\nu}^{T,L}$ are defined by

$$P_{ij}^T = \delta_{ij} - \hat{q}_i \hat{q}_j, \quad P_{00}^T = P_{0i}^T = 0, \quad (11)$$

$$P_{\mu\nu}^L = -g_{\mu\nu} + \frac{q_\mu q_\nu}{q^2} P_{\mu\nu}^T. \quad (12)$$

It contains the gauge parameter ξ , which must not appear in physical results. In the weak coupling limit, q_0 is small as compared to $|\vec{q}|$. In this case we can expand the projectors $P_{\mu\nu}^L \simeq \delta_{\mu 0} \delta_{\nu 0}$ and $q_i q_j / q^2 \simeq \hat{q}_i \hat{q}_j$. The gap equation now becomes

$$\Delta_1(k_0) = \frac{2g^2}{3} \int \frac{d^4q}{(2\pi)^4} \left\{ \frac{\Delta_1(q_0)}{q_0^2 - (|\vec{q}| - \mu)^2 - \Delta_1(q_0)^2} \left(\frac{\frac{3}{2} - \frac{1}{2} \hat{k} \cdot \hat{q}}{(k - q)^2 - G} + \frac{\frac{1}{2} + \frac{1}{2} \hat{k} \cdot \hat{q}}{(k - q)^2 - F} \right) \right. \\ \left. + \frac{\Delta_2(q_0)}{q_0^2 - (|\vec{q}| + \mu)^2 - \Delta_2(q_0)^2} \left(\frac{\frac{1}{2} + \frac{1}{2} \hat{k} \cdot \hat{q}}{(k - q)^2 - G} + \frac{\frac{1}{2} - \frac{1}{2} \hat{k} \cdot \hat{q}}{(k - q)^2 - F} + \frac{\xi}{(q - k)^2} \right) \right\}. \quad (13)$$

There is a similar equation for Δ_2 in which the two terms in the round brackets are interchanged. Only the first term in (13) has a singularity on the Fermi surface. In the

weak coupling limit, we can therefore drop the second term, and we are left with an equation for $\Delta(p_0) \equiv \Delta_1(p_0)$. This equation is independent of the gauge parameter ξ . The second gap parameter Δ_2 is not suppressed in magnitude. However, Δ_2 does not lead to a gap on the Fermi surface, and its value is gauge dependent.

We should note that the fact that the gap is gauge independent in the present weak-coupling approximation is a consequence of the fact that the gap is determined by the scattering of quarks that are almost on shell. For on-shell quarks, the fact that the gauge dependent part of the propagator does not contribute follows directly from the equations of motion for the quark fields.

For large chemical potential the integral over q is dominated by momenta in the vicinity of the Fermi surface, $|\vec{q}| \simeq \mu$ and $q_0 \ll \mu$. We can expand all momenta as $\vec{q} = \vec{q}_F + \vec{l}$, where \vec{q}_F is on the Fermi surface, and \vec{l} is orthogonal to it. Asymptotically, $|\vec{l}| \ll |\vec{q}_F|$ and the integration measure becomes $dq_0 \mu^2 dl d \cos \theta d\phi$. We also have $|\vec{q} - \vec{k}| \simeq \sqrt{2}\mu(1 - \cos \theta)$. The integral over ϕ is performed trivially, and the integral over \vec{l} is done by picking up the pole in the diquark propagator. We find

$$\Delta(p_0) = \frac{g^2}{12\pi^2} \int dq_0 \int d \cos \theta \left(\frac{\frac{3}{2} - \frac{1}{2} \cos \theta}{1 - \cos \theta + (G - (p_0 - q_0)^2)/(2\mu^2)} + \frac{\frac{1}{2} + \frac{1}{2} \cos \theta}{1 - \cos \theta + (F - (p_0 - q_0)^2)/(2\mu^2)} \right) \frac{\Delta(q_0)}{\sqrt{q_0^2 + \Delta(q_0)^2}}. \quad (14)$$

The integral over $\cos \theta$ is dominated by small θ , corresponding to almost collinear scattering. It is therefore important to take medium modifications of the gluon propagator at small momenta into account. For $\vec{q} \rightarrow 0$ and to leading order in perturbation theory we have

$$F = 2m^2, \quad G = \frac{i\pi}{2} m^2 \frac{q_0}{|\vec{q}|} \Theta(\vec{q}^2 - q_0^2), \quad (15)$$

with $m^2 = N_f g^2 \mu^2 / (4\pi^2)$. In the longitudinal part, $m_D^2 = 2m^2$ is the familiar Debye screening mass. In the transverse part, there is no screening of static modes, but nonstatic modes are dynamically screened due to Landau damping. In our case, typical frequencies are on the order of the gap, $q_0 \simeq \Delta$. This means that the electric part of

the interaction is screened at $q_E \simeq m_D^{1/2}$ whereas the magnetic interaction is screened at $q_M \simeq (\pi/4 \cdot m_D^2 \Delta)^{1/3}$.

Asymptotically, $q_M \ll q_E$, and magnetic gluon exchange dominates over electric gluon exchange. We therefore begin by analyzing the gap equation taking into account the magnetic part of the interaction only. We will also approximate $\cos \theta \simeq 1$ in the denominator and drop $(q_0 - p_0)^2$ in the denominator. All of these terms will be reinstated later. The integration over $\cos \theta$ is now straightforward. Analytically continuing to imaginary q_0 we have

$$\Delta(p_0) = \frac{g^2}{18\pi^2} \int dq_0 \log \left(1 + \frac{64\pi\mu}{N_f g^2 |p_0 - q_0|} \right) \frac{\Delta(q_0)}{\sqrt{q_0^2 + \Delta(q_0)^2}}. \quad (16)$$

If we are only interested in the leading exponential behavior of the gap we can drop the numerical factors and the powers of g in the logarithm. We then arrive at

$$\Delta(p_0) = \frac{g^2}{18\pi^2} \int dq_0 \log \left(\frac{\mu}{|p_0 - q_0|} \right) \frac{\Delta(q_0)}{\sqrt{q_0^2 + \Delta(q_0)^2}}, \quad (17)$$

which is the equation discussed in the appendix of Son's paper [6]. This equation was derived from the on-shell quark-quark scattering amplitude. What we have shown here is that one can indeed derive this equation from the Dyson-Schwinger equation in the weak coupling limit, and that the result is independent of the gauge parameter. Son also derives an approximate solution to this integral equation,

$$\Delta_{\text{app.}}(p_0) \equiv \Delta_0 \sin \left(\frac{g}{3\sqrt{2}\pi} \log \left(\frac{\mu}{p_0} \right) \right), \quad p_0 > \Delta_0, \quad (18)$$

with $\Delta_0 = \mu \exp(-3\pi^2/(\sqrt{2}g))$. The approximations involved are expected to reproduce the correct coefficient in the exponent, but do not fix the prefactor.

3. We have therefore solved the Eliashberg equation (17) numerically for different chemical potentials. We have used the one-loop running coupling constant evaluated at the Fermi momentum $p_F = \mu$. This is an average over the momenta of the exchanged gluons, which are in the range $[q_M, 2\mu]$. Without a higher order calculation one cannot fix the scale in the running coupling. We will see that the preexponential factor in the final result behaves as g^{-5} . This factor is almost optimal to give a remarkably weak scale dependence.

The result for the function $\Delta(p_0)$ for $\mu = 400$ MeV and $\mu = 10^{10}$ MeV is shown in Fig. 1. The solid line is the numerical result while the dashed line shows the approximate solution (18), rescaled by an overall factor c , $\Delta(p_0) = c\Delta_{\text{app.}}(p_0/c)$. At $\mu = 10^{10}$ MeV, $g \simeq 0.67$ and Son's solution is in excellent agreement with the exact result, up to an overall factor $c \simeq 2$. At $\mu = 400$ MeV the coupling is significantly bigger than 1, $g \simeq 3.43$, but the approximate solution is still qualitatively correct.

The scaling of the maximum gap with the chemical potential is shown in Fig. 2. The solid line is the numerical result and the dashed lines correspond to $cg^{-k}\mu \exp(-3\pi^2/(\sqrt{2}g))$ with $k = 0, \dots, 5$. We observe that the $k = 0$ curve provides an excellent fit to the data even for small chemical potentials. Again, the overall coefficient is $c \simeq 2$.

Let us make a few observations at this point. First, we note that the use of perturbation theory to determine the dynamic screening is self consistent. Since $\Delta \sim \mu \exp(-\text{const.}/g)$, the gap grows as $\mu \rightarrow \infty$ and $q_M \gg \Lambda_{QCD}$. Second, we note that it is essential to keep the frequency dependence of the gap. For small frequencies $\Delta(p_0)$ varies over scales on the order of $p_0 \sim \Delta_0$ itself. Therefore, $\Delta(p_0)$ cannot be replaced by a constant. Were we to approximate $\Delta(p_0) \simeq \Delta_0$, as in [13], we would obtain a gap equation for Δ_0 that has the correct double logarithmic structure and gives $\Delta_0 \simeq \mu \exp(-\text{const.}/g)$, but the constant in the exponent would not be correct.

Finally, we note that it is easy to see what taking into account the numerical coefficients and the factor g^2 in equation (16) will do. Any numerical factor inside the logarithm can be absorbed by rescaling the frequencies. Therefore, if $\Delta_{\text{app.}}(p_0)$ in (18) is an approximate solution to (17), then $\Delta'(p_0) = c\Delta_{\text{app.}}(p_0/c)$ with $c = 64\pi/(N_f g^2)$ is an approximate solution to (16). This can also be seen from Figs. 3 and 4 where we show the numerical solution to the Eliashberg equation (16) for the superconducting gap from magnetic gluon exchanges. Asymptotically, the solution is well described by the function $\Delta'(p_0)$ with $c \simeq 175g^{-2}$.

We now come to the role of electric gluon exchanges. We include the second term in (14) with $F = m_D^2$. We again use the approximation $\cos \theta \simeq 1$ in the numerator and drop the $(q_0 - p_0)^2$ term in the denominator. Let us note that in the forward direction, electric and

magnetic gluon exchanges have the same overall factor. Performing the integral over $\cos\theta$, we find

$$\Delta(p_0) = \frac{g^2}{18\pi^2} \int dq_0 \left\{ \log \left(1 + \frac{64\pi\mu}{N_f g^2 |p_0 - q_0|} \right) + \frac{3}{2} \log \left(1 + \frac{8\pi^2}{N_f g^2} \right) \right\} \frac{\Delta(q_0)}{\sqrt{q_0^2 + \Delta(q_0)^2}}, \quad (19)$$

where the factor 3/2 in front of the second term comes from the difference between dynamic screening, $q_M \sim |\vec{q}|^{1/3}$, and static screening, $q_E \sim |\vec{q}|$. In the weak coupling limit we again expect the solution to be of the form $c\Delta_{\text{app}}(p_0/c)$ with

$$c = 1024\sqrt{2}\pi^4 N_f^{-5/2} g^{-5} = 256\pi^4 \simeq 2.5 \cdot 10^4 \quad (N_f = 2). \quad (20)$$

We can compare this prediction to our numerical results, obtained from solving (14). In this equation, we take into account both electric and magnetic gluon exchanges. We also keep the $\cos\theta$ dependence in the numerator, and the terms $(q_0 - p_0)^2$ in the denominator. Finally, we take into account that extremely collinear exchanges with $|\vec{q}| < q_0$ are not dynamically screened. The numerical results are shown in Figs. 5 and 6. Asymptotically, the gap is well described by $c\Delta_{\text{app}}(p_0/c)$ with $c \simeq 2.6 \cdot 10^4 g^{-5}$. We notice that for $\mu = 10^{10}$ MeV the solution has a ‘knee’ at $p_0 \simeq 10^9$ MeV. This comes from the fact that for frequencies $p_0 > \sqrt{N_f/(8\pi)}g\mu$ the retardation terms $\sim (p_0 - q_0)^2$ dominate over screening. In this regime, the solution is of the same form, but the scale factor is different.

Overall, the scaling with $g^{-5} \exp(-3\pi^2/(\sqrt{2}g))$ is clearly visible, though not quite as impressively as in the case with magnetic gluon exchange only. For chemical potentials that are of physical interest, $\mu < 1000$ MeV, the gap reaches $\Delta_0 \simeq 100$ MeV. We should caution, however, that in this regime $g \simeq (2-4)$, and higher order corrections are probably important. Nevertheless, it is gratifying to see that the order of magnitude of the result agrees with previous calculations [10,11] based on more phenomenological effective interactions, which were normalized to the strength of chiral symmetry breaking at zero density, rather than the calculable asymptotics of the running coupling.

4. There are a number of questions that will need to be addressed in a more complete calculation. First, we have concentrated on the case $N_f = 2$. For $N_f = 3$, there are two order

parameters, corresponding to the color antisymmetric and color symmetric components of the color-flavor locked state. This is only a minor complication, since the color symmetric component is suppressed in the weak coupling limit.

A more complicated issue is the role of the Meissner effect. For $N_f = 2$, the dominant order parameter only breaks color $SU(3) \rightarrow SU(2)$, and all gluons that contribute to pairing, except for one, live in the unbroken part of the gauge group. In the case of $N_f = 3$, the Higgs mechanism is complete and all gluons acquire a mass. At zero momentum and frequency, the screening mass is on the order of $m^2 \sim g^2 \mu^2$, much larger than the dynamic screening scale q_M . At finite momentum transfer, on the other hand, the screening mass is $m^2 \sim g^2 \mu^2 \Delta / |\vec{q}|$ [14], which is of the same form as the dynamic screening effect. The Meissner effect will therefore not affect the dependence of the gap on the coupling constant, but it will affect the numerical coefficient.

Finally, one has to address higher order corrections to the perturbative result. In particular, one would like to know what the functional form of the corrections is, and whether the applicability of perturbation theory requires $g < 1$, or some weaker condition like $g < \pi$. We have already mentioned wave function renormalization as one source of higher order correction [6]. Another issue is vertex corrections. The vertex correction generated by hard dense loops is [15]

$$\Gamma_\mu^a(p_1, p_2) = g \frac{\lambda^a}{2} \left(\gamma_\mu - m_f^2 \int \frac{d\Omega}{4\pi} \frac{\hat{K}_\mu \gamma \cdot \hat{K}}{(p_1 \cdot \hat{K})(p_2 \cdot \hat{K})} \right), \quad (21)$$

where $\hat{K} = (i, \hat{k})$ is a light like vector and $m_f^2 = g^2 \mu^2 / (6\pi^2)$. We can insert this correction into the gap equation (9). We find that the coefficient of the magnetic gluon exchange is modified as

$$\left(\frac{3}{2} - \frac{1}{2} \cos \theta \right) \rightarrow \left(\frac{3}{2} - \frac{1}{2} \cos \theta \right) + \frac{m_f^2}{\mu^2} + \frac{1}{2} (1 - \cos \theta) m_f^2 \int \frac{d\Omega}{4\pi} \frac{1}{(p \cdot \hat{K})(q \cdot \hat{K})}. \quad (22)$$

In the forward direction $\cos \theta \simeq 1$, which dominates the gap equations, this is just a higher order correction. Vertex corrections have a (μ/q_0) enhancement in the backward direction $\cos \theta \simeq -1$, but the integral over $\cos \theta$ is finite as $q_0 \rightarrow 0$. Vertex corrections in the magnetic

part therefore do not modify the asymptotic form of the gap. The same is true for vertex corrections in the electric part of the interaction.

5. In summary, we have performed a perturbative calculation of the superconducting gap in two flavor QCD at very high density. We find that the gap scales as $\Delta_0 \simeq 256\pi^4\mu g^{-5} \exp(-3\pi^2/(\sqrt{2}g))$, where the overall coefficient is correct up to a factor of order one. In the physically interesting regime $\mu < 1$ GeV, the gap is on the order of 100 MeV, in agreement with earlier calculations based on instantons or schematic interactions adjusted to the size of the chiral condensate at zero density.

Acknowledgements: We would like to thank D. Son and K. Rajagopal for useful discussions.

REFERENCES

- [1] S. C. Frautschi, Asymptotic freedom and color superconductivity in dense quark matter, in: Proceedings of the Workshop on Hadronic Matter at Extreme Energy Density, N. Cabibbo, Editor, Erice, Italy (1978)
- [2] F. Barrois, Nucl. Phys. B129, 390 (1977)
- [3] M. Alford, K. Rajagopal, and F. Wilczek, Nucl. Phys. **B537**, 443 (1999).
- [4] T. Schäfer and F. Wilczek, Phys. Rev. Lett. **82**, 3956 (1999).
- [5] D. Bailin and A. Love, Phys. Rept. **107**, 325 (1984).
- [6] D. T. Son, Phys. Rev. **D 59**, 094019 (1999); hep-ph/9812287.
- [7] T. Schäfer and F. Wilczek, Phys. Lett. **B450**, 325 (1999); hep-ph/9810509.
- [8] N. Evans, S. Hsu, and M. Schwetz, Nucl. Phys. **B551**, 275 (1999) and Phys. Lett. **B449**, 281 (1999).
- [9] R. D. Pisarski, D. H. Rischke, preprint, nucl-th/9811104.
- [10] M. Alford, K. Rajagopal, and F. Wilczek, Phys. Lett. **B422**, 247 (1998).
- [11] R. Rapp, T. Schäfer, E. V. Shuryak, and M. Velkovsky, Phys. Rev. Lett. **81**, 53 (1998).
- [12] R. D. Pisarski, D. H. Rischke, preprint, nucl-th/9903023.
- [13] D. K. Hong, preprints, hep-ph/9905523 and hep-ph/9812510.
- [14] A. A. Abrikosov, L. P. Gorkov, and I. E. Dzyaloshinski, *Methods of Quantum Field Theory in Statistical Physics*, Prentice Hall, Englewood Cliffs, New Jersey 1963.
- [15] M. LeBellac, *Thermal Field Theory*, Cambridge University Press, Cambridge 1996.

FIGURES

FIG. 1. Solution of the Eliashberg equation (17) as a function of imaginary frequency q_0 . The upper and lower panels show the solution for $\mu = 400$ MeV and $\mu = 10^{10}$ MeV, respectively. The solid lines show the numerical solution and the dashed lines shows the approximate solution (18), scaled to the same value of the gap.

FIG. 2. Dependence of the gap on the chemical potential for the solution of the Eliashberg equation (17). Here, $g(\mu)$ is taken to run according to the one-loop beta function. The dotted curves show the functions $g^{-k} \exp(-(3\pi^2)/(\sqrt{2}g))$ for $k = 0$ (top), $\dots, 5$ scaled to the value of the gap at the maximum chemical potential.

FIG. 3. Same as figure 1 for the solution of the Eliashberg equation with magnetic gluon exchange only, see equ. (16).

FIG. 4. Same as figure 2 for the solution of the Eliashberg equation with magnetic gluon exchange only.

FIG. 5. Same as figure 1 for the solution of the Eliashberg equation with magnetic and electric gluon exchanges, see equ. (14).

FIG. 6. Same as figure 2 for the solution of the Eliashberg equation with magnetic and electric gluon exchanges.

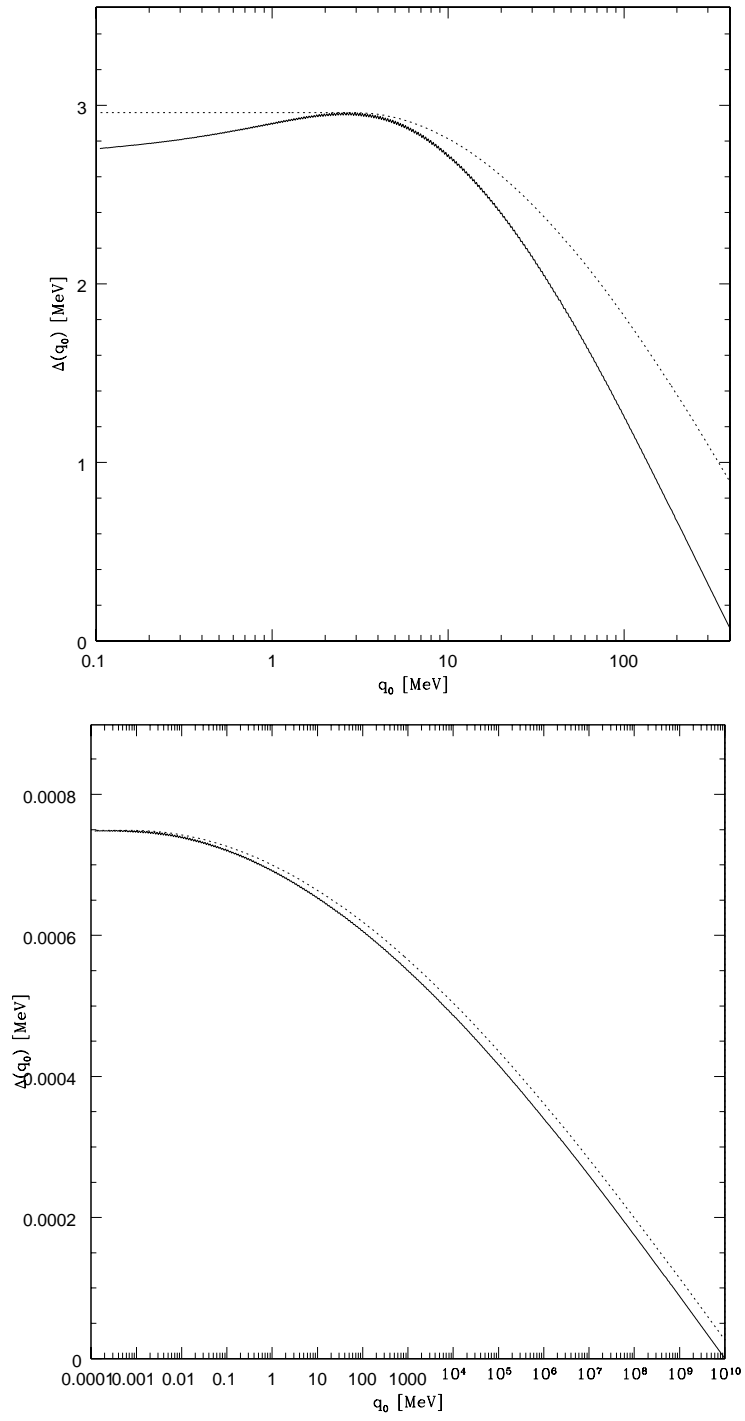


FIG. 1.

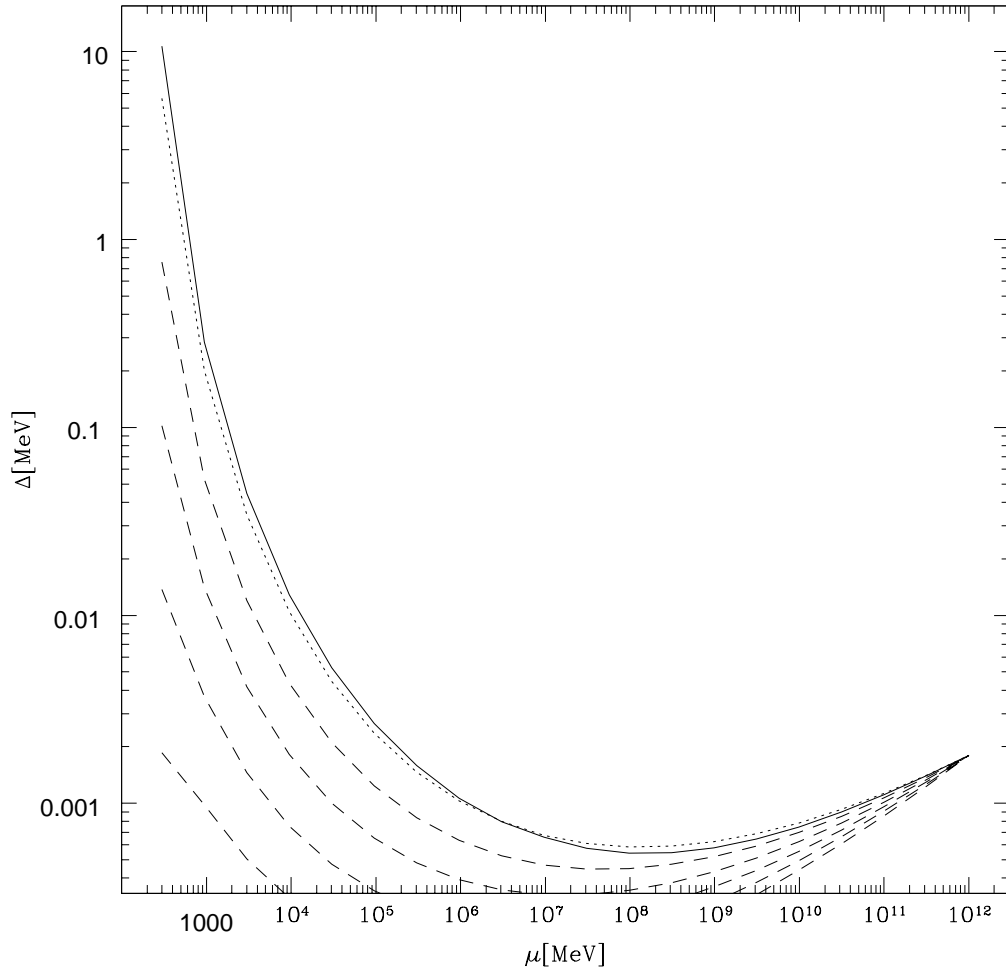


FIG. 2.

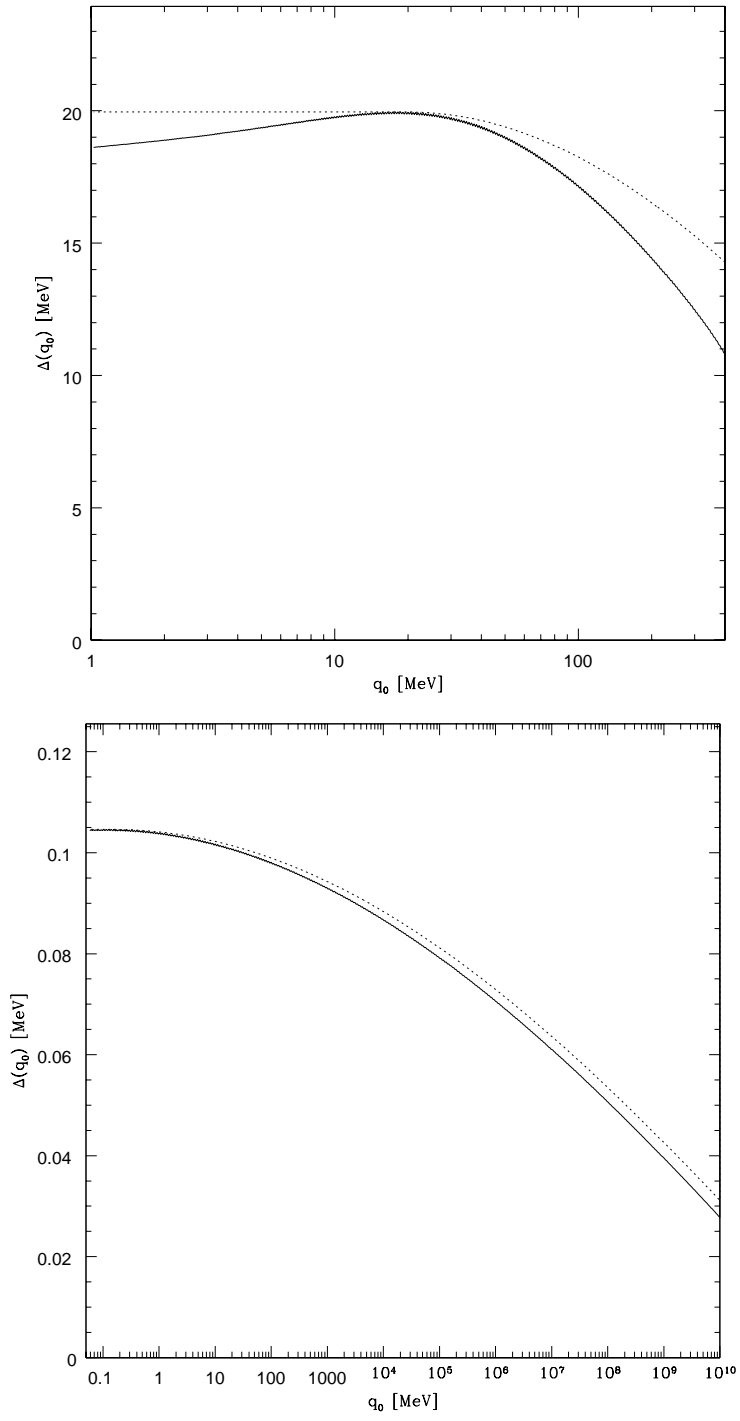


FIG. 3.

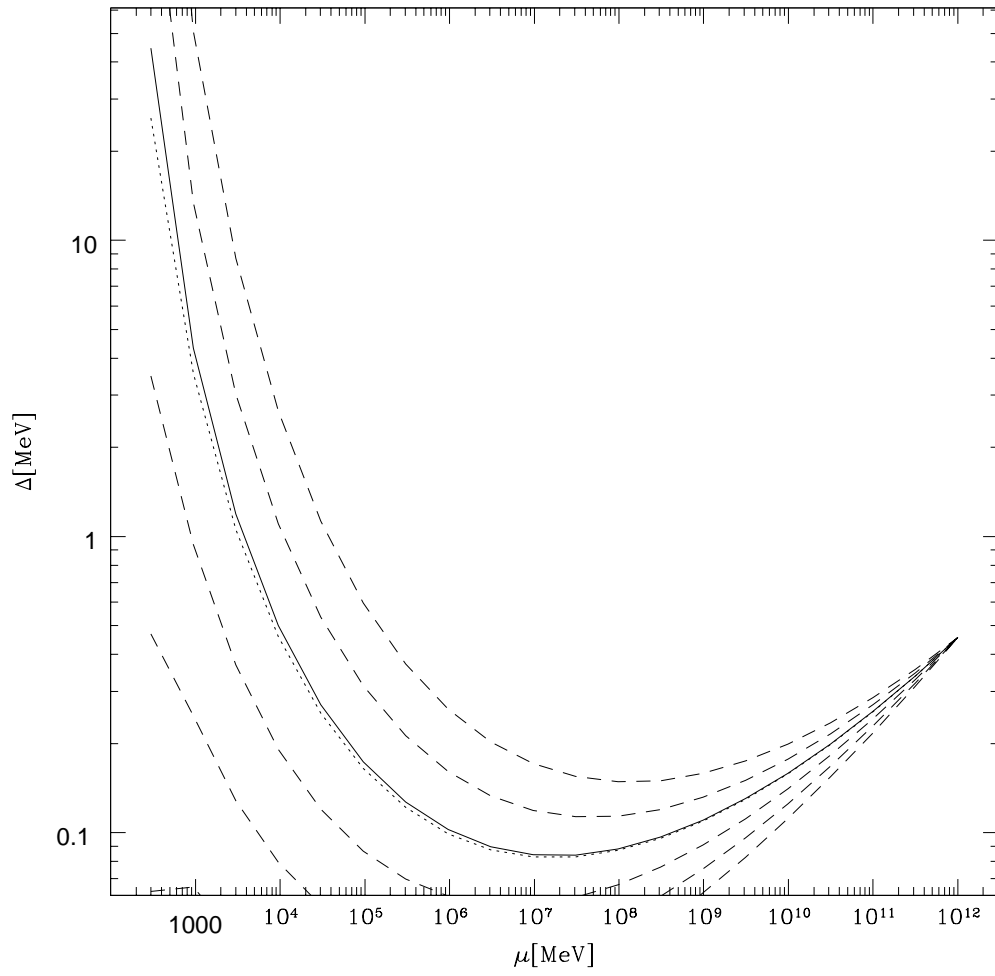


FIG. 4.

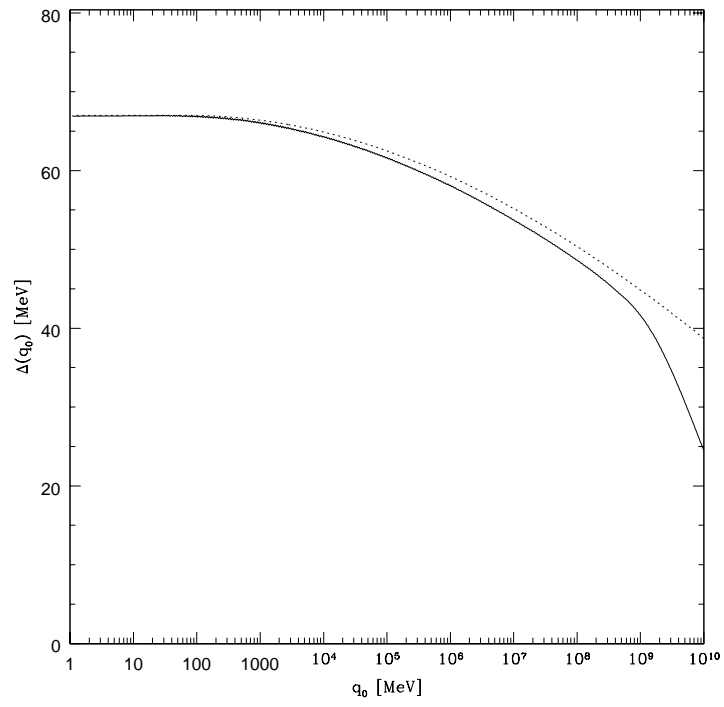
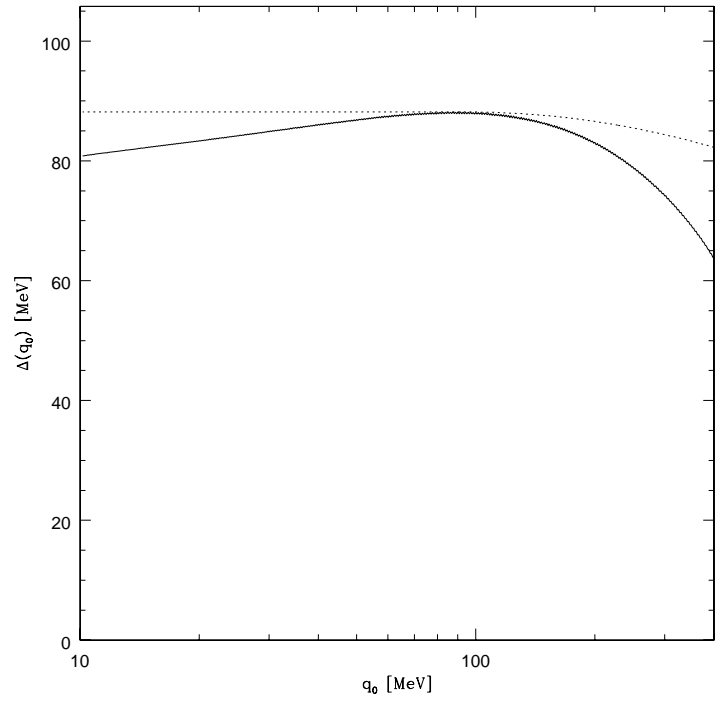


FIG. 5.

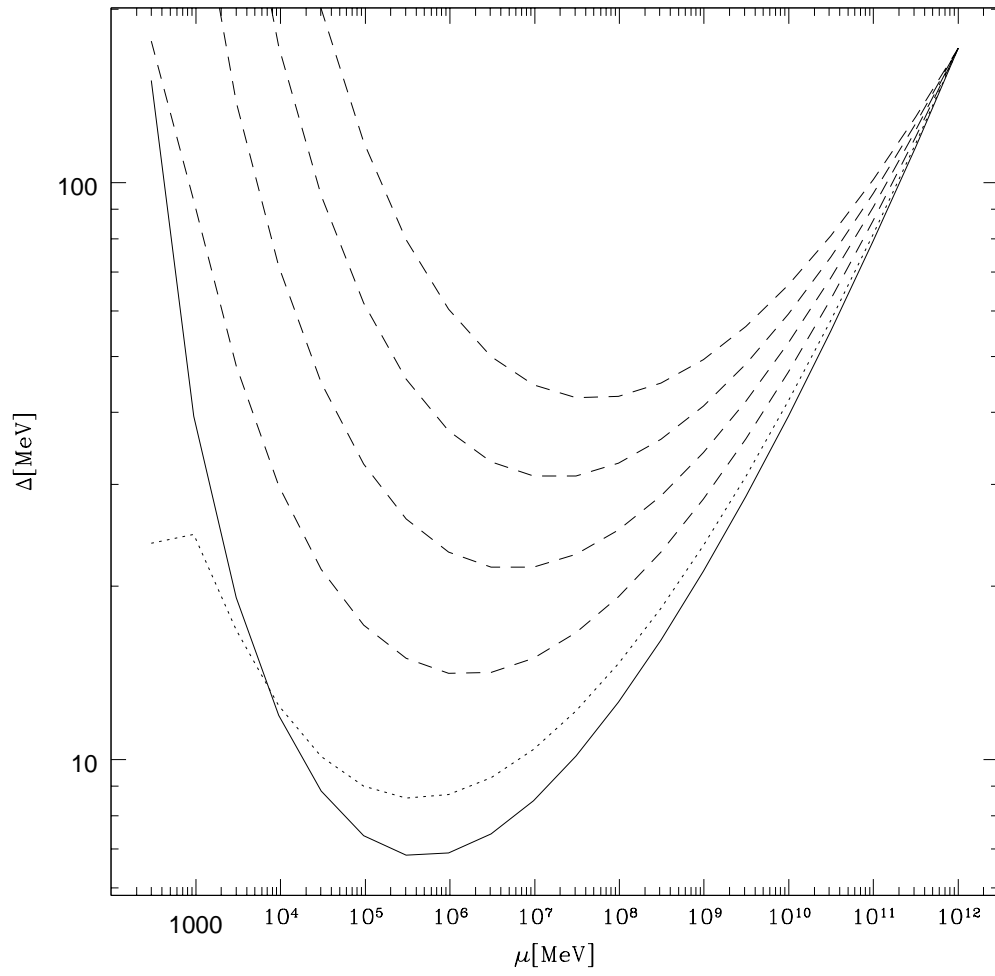


FIG. 6.